RESEARCH ARTICLE

CrossMark

Influence of Temperature on the Performance of Forward Osmosis Using Ammonium Bicarbonate as Draw Solute

Liyuan Feng[1,2,3] · Lixin Xie[1,2,3] · Gaofeng Suo[1,2,3] · Xiaofeng Shao[1,2,3] · Tao Dong[1,2,3]

Abstract

This study investigated the influence of temperature on the performance of forward osmosis (FO) under the condition that the feed solution (FS) temperature was different from draw solution (DS) temperature. An FO model considering the mass and heat transfer between FS and DS was developed, and the FO experiment with ammonium bicarbonate solution as DS and sodium chloride solution as FS was carried out. The predicted water flux and reverse draw solute flux using the developed model coincided with the experimental fluxes. Increases in the temperature of FS or DS yield corresponding increases in the water flux, reverse draw solute flux, and forward rejection of feed solute. Compared with increasing the FS temperature, increasing the DS temperature has a more significant impact on enhancing FO performance. When the temperature of DS increased from 20 to 40 °C, the specific reverse solute flux decreased from 0.231 to 0.190 mol/L.

Keywords Forward osmosis · Modeling · Temperature · Mass transfer · Heat transfer

Introduction

Seawater desalination is considered to be one of the most attractive technologies for alleviating water scarcity [1]. However, conventional desalination methods such as reverse osmosis (RO), electrodialysis, and thermal distillation are energy intensive. To improve energy efficiency, an emerging technology named forward osmosis (FO) has been developed. FO utilizes the natural osmotic pressure difference to drive the transport of water molecules from feed solution (low osmotic pressure) to draw solution (high osmotic pressure), thereby eliminating the need for additional hydraulic pressure. Compared with typical pressure-driven technologies, FO presents several advantages, including less energy consumption, low membrane fouling, and high salt rejection [2]. FO has been applied in the treatment of oil-sands

tailings water [3], water reuse [4], fertilizer-drawn forward osmosis desalination [5], and concentrated liquid foods [6].

Temperature is a key factor on the performance of FO. On the one hand, it influences solution physicochemical properties such as diffusion coefficient, density, viscosity, and osmotic pressure. On the other hand, temperature also affects the performance of FO membrane. Some research about the influence of temperature on FO has been conducted. Zhao and Zou [7] investigated the effects of temperature on water flux, recovery, concentration factor, and membrane scaling. It was found that the water flux, recovery, and concentration factor increased with an increase in temperature, but a higher temperature caused more severe membrane scaling. Nematzadeh et al. [8] evaluated the effect of temperature on the performance of FO using sodium bicarbonate as draw solute and found that water flux and the reverse draw solute flux increased with increases in temperature.

However, the above research was carried out under the condition that the temperatures of feed solution (FS) and draw solution (DS) were the same. In practical desalination applications, a temperature difference between FS and DS is inevitable because the temperature of seawater is affected by sea latitude, vertical depth, and surrounding climate. To date, only a few studies have investigated the impact of temperature on FO when there is a temperature difference between FS and DS. Phuntsho et al. [9] investigated the influence of

✉ Lixin Xie
  xie_lixin@tju.edu.cn

1 School of Chemical Engineering and Technology, Tianjin University, Tianjin 300072, China

2 Tianjin Key Laboratory of Membrane Science and Desalination Technology, Tianjin 300072, China

3 Collaborative Innovation Center of Chemical Science and Engineering, Tianjin 300072, China

temperature difference on water flux using potassium chloride as draw solute, and found that only increasing the DS temperature had a greater impact than only increasing the FS temperature. Hawari et al. [10] investigated the effects of FS and DS temperatures on water flux and found that water flux increased when the DS temperature increased from 20 to 26 °C, and decreased when above 26 °C due to thermo-osmosis. Besides water flux, there are other factors, such as reverse draw solute flux, forward rejection of feed solute, and specific reverse solute flux, related to FO performance. Investigating the changes in water flux, reverse draw solute flux, forward rejection of feed solute, and specific reverse solute flux with temperature is needed for comprehensively evaluating the impact of temperature on FO performance when the temperatures of FS and DS are different.

When the temperatures of FS and DS are different, heat transfer occurs across the FO membrane and boundary layers, which causes temperature alteration and impacts the FO performance. The focus of previous FO models is only mass transfer between FS and DS, and only the study by You et al. [11] modeled the FO process considering heat transfer. This model was used to predict the water flux, while it neglected the influence of draw solute reverse permeation, which played a significant role in water flux drop [12]. We revised the FO model considering the impact of draw solute reverse permeation, and the revised model could predict not only water flux, but also reverse draw solute flux.

Ammonium bicarbonate, which meets the requirements for an appropriate draw solute, i.e., high solubility, low viscosity, non-toxicity and low cost, is widely employed in FO. In comparison with other inorganic draw solutes, ammonium bicarbonate can be easily decomposed into carbon dioxide and ammonia gas upon heating. In the NH_4HCO_3 FO pilot process [13], the required water can be obtained by distillation, and the ammonium bicarbonate can then be recycled by absorption. Thus, the temperature of DS is different from that of FS. Investigating the influence of temperature on the performance of the NH_4HCO_3 FO process with the temperatures of FS and DS being different is significant. To the best of our knowledge, however, study about the effect of temperature on the performance of NH_4HCO_3 FO process with the temperatures of FS and DS being different is very scarce.

Theory

As shown in Fig. 1, there are three mass transfer processes in FO. First, water molecules in FS diffuse into bulk DS. Next, the feed solutes permeate into bulk DS due to the limited rejection of FO membrane. Thirdly, the draw solutes permeate into bulk FS for the same reason. When there is a temperature difference between FS and DS, heat current
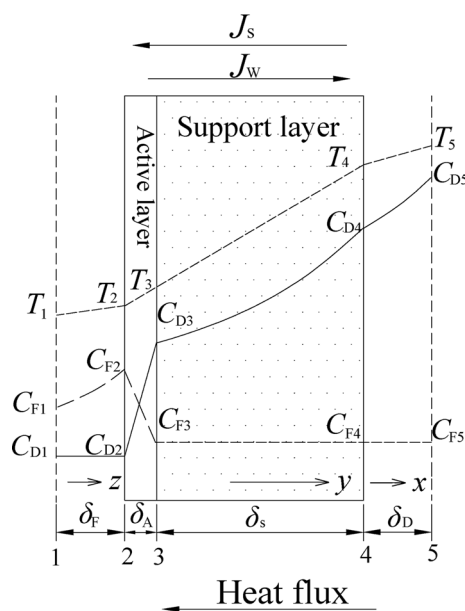
Fig. 1 Schematic diagram of FS and DS temperature and concentration gradients across FO membrane (the active layer faces FS)

is transferred from the high-temperature side to the low-temperature side.

Mass Transfer

Forward Water Flux

According to the solution–diffusion theory, the water flux through the active layer of an FO membrane is determined by the effective osmotic pressure difference across the active layer, which is given by the following equation [2]:

$$J_w = A(\pi_{D3} - \pi_{F2}) \tag{1}$$

where J_w is the water flux (L/(m^2 h)); A is the water permeation coefficient of FO membrane (L/(m^2 h MPa)), as determined by the method reported in [14]; π is the osmotic pressure (MPa); the subscripts D, F refer to DS, FS, respectively; and variables with the subscript 2 or 3 are at the surface of active layer or the interface between active layer and support layer, respectively.

The solution osmotic pressure can be calculated using Van't Hoff's equation, that is

$$\pi = nCRT \tag{2}$$

where n is the number of solute ions dissolved in solution; C is the concentration (mol/L); T is the temperature (K); and R is the gas constant, which is 8.314×10^{-3} kJ/(mol K).

Reverse Draw Solute Flux

The reverse draw solute flux, J_s, is related to the DS concentration gradient across active layer, which can be written as follows [15]:

$$J_s = B(C_{D3} - C_{D1}) \tag{3}$$

where J_s is the reverse draw solute flux (mol/(m^2 h)); B is the draw solute permeation coefficient of the FO membrane (L/(m^2 h)), as determined by the method reported in [14]; and the variable with the subscript 1 denotes its presence in bulk FS.

Concentrative External Concentration Polarization (CECP)

Like the majority of pressure-driven membrane processes [16], feed solutes are retained on the active layer surface as water molecules flow to DS, which causes CECP. The concentration of FS on the active layer surface can be expressed by the following equation [17]:

$$C_{F2} = \frac{C_{F1}e^{Pe_F}}{R_F + (1 - R_F)e^{Pe_F}} \tag{4}$$

$$Pe_F = \frac{3,600,000J_w}{k_F} = 3,600,000J_w\frac{\delta_F}{D_F} = 3,600,000J_w\frac{d_F}{Sh_FD_F}$$

where R_F is the forward rejection of feed solute; Pe [18] is the Peclet number; k is the mass transfer coefficient (m/s); δ_F is the thickness of FS boundary layer (m); D is the diffusion coefficient (m^2/s); d is the hydraulic diameter ($d = 2H$ [19], H is the channel height); and Sh [18] is the Sherwood number, which is calculated as follows:

$$Sh_F = 1.85\left(Re_F Sc_F \frac{d_F}{L_F}\right)^{0.33} \text{(Laminar boundary layer)} \tag{5}$$

$$Sh_F = 0.04Re_F^{0.75}Sc_F^{0.33} \text{ (Turbulent boundary layer)} \tag{6}$$

where Re is the Reynolds number; L is the channel length (m); Sc is the Schmidt number, as calculated by $Sc = \frac{\mu}{\rho D}$, and μ and ρ are the dynamic viscosity (kg/(m s)) and density (kg/m^3), respectively.

The diffusion coefficients of sodium chloride solution can be obtained from Refs. [20, 21].

Internal Concentration Polarization (ICP)

In FO process, the draw solutes diffuse inside the porous support layer, which causes the draw solution concentration at the interface between active layer and support layer to be lower than that at the support layer surface, as is known as ICP. The reverse draw solute flux inside the support layer under steady-state conditions can be written as follows [12]:

$$J_s = -J_w C_D + D_{De}\frac{dC_D}{dy} \tag{7}$$

where D_{De} is the effective diffusion coefficient of DS in support layer, and is proportional to D_{D5} by $D_{De} = \frac{D_{D5}\varepsilon}{\tau}$, and ε and τ are the porosity (%) and tortuosity of support layer, respectively.

By integrating Eq. (7) across the support layer thickness (δ_s) at $y = 0$, $C_D = C_{D3}$ and $y = \delta_s$, $C_D = C_{D4}$

$$C_{D3} = \left(C_{D4} + \frac{J_s}{J_w}\right)e^{(-Pe_{D34})} - \frac{J_s}{J_w} \tag{8}$$

w h e r e $Pe_{D34} = 3,600,000J_wK = 3,600,000J_w\frac{\delta_s}{D_{De}} = 3,600,000J_w\frac{S}{D_{D5}}$, K [12] is the solute resistivity coefficient (s/m); and S is the structural parameter of support layer (m), which can be calculated as follows [22]:

$$S = \frac{\delta_s\tau}{\varepsilon} = \left(\frac{D_{D5}}{J_w}\right)\ln\frac{B + A\pi_{D5}}{B + J_w}. \tag{9}$$

The diffusion coefficients of ammonium bicarbonate solution can be obtained from Ref. [23].

Dilutive External Concentration Polarization (DECP)

The DS is diluted with solute diffusion and water permeation on the surface of support layer, as known as DECP. The reverse draw solute flux in the boundary layer can be written in the same expression as Eq. (7) under the following boundary conditions:

$$\begin{cases} x = 0, \ C_D = C_{D4} \\ x = \delta_D, \ C_D = C_{D5} \end{cases}$$

where δ_D is the thickness of DS boundary layer; and the subscript 4 or 5 denotes their presence at the surface of support layer or in bulk DS, respectively. C_{D4} can be expressed as follows:

$$C_{D4} = e^{-Pe_D}\left(C_{D5} + \frac{J_s}{J_w}\right) - \frac{J_s}{J_w} \tag{10}$$

Heat Transfer

As shown in Fig. 1, heat transfer occurs when there is a temperature difference between FS and DS, which can be described by the following equations:

$$Q_F = h_F(T_2 - T_1) \tag{11}$$

$$Q_D = h_D(T_5 - T_4) \tag{12}$$

$$Q_a = h_a(T_3 - T_2) - 3{,}600{,}000(c_{\rho w}J_w\rho_w - c_{\rho D}J_sM_D)(T_3 - T_2) \tag{13}$$

$$Q_s = h_s(T_4 - T_3) - 3{,}600{,}000(c_{\rho w}J_w\rho_w - c_{\rho D}J_sM_D)(T_4 - T_3) \tag{14}$$

where Q represents the heat flux (W/m^2); h is the heat transfer coefficient (W/(m^2 K)); M is the molar mass (g/mol); c_ρ is the specific heat (J/(kg K)); and the subscripts w, a, and s refer to water, the active layer and support layer of FO membrane, respectively.

The specific heats of NH_4HCO_3 at different temperatures can be obtained from Refs. [20, 23, 24].

According to the heat transfer theory, heat transfer remains the same across the FS boundary layer, the active layer, the support layer and the DS boundary layer. Therefore, the temperatures on the surface of active layer, the interface between active layer and support layer and the surface of support layer can be obtained by combining Eqs. (11–14):

$$T_2 = \frac{h_F T_1 + T_3(h_a - 3{,}600{,}000(c_{\rho w}J_w\rho_w - c_{\rho D}J_sM_{D5}))}{h_F + (h_a - 3{,}600{,}000(c_{\rho w}J_w\rho_w - c_{\rho D}J_sM_{D5}))} \tag{15}$$

$$T_3 = \frac{h_s T_4 + h_a T_2 - (T_4 + T_2)(3{,}600{,}000(c_{\rho w}J_w\rho_w - c_{\rho D}J_sM_{D5}))}{h_a + h_s - 2 \times 3{,}600{,}000(c_{\rho w}J_w\rho_w - c_{\rho D}J_sM_{D5})} \tag{16}$$

$$T_4 = \frac{h_D T_5 + T_3(h_s - 3{,}600{,}000(c_{\rho w}J_w\rho_w - c_{\rho D}J_sM_{D5}))}{h_D + (h_s - 3{,}600{,}000(c_{\rho w}J_w\rho_w - c_{\rho D}J_sM_{D5}))} \tag{17}$$

Heat transfer coefficient is presented by Babu et al. [25]:

$$h = \frac{\lambda Nu}{d_h} \tag{18}$$

$$h_a = \frac{\lambda_a}{\delta_a} \tag{19}$$

$$h_s = \frac{\varepsilon\lambda_w + (1 - \varepsilon)\lambda_s}{\delta_s} \tag{20}$$

where λ is the thermal conductivity (W/(m K)); δ_a is the thickness of active layer (m); and Nu is the Nusselt number, calculated by Babu et al. [25]:

$$Nu = 0.332Re^{4/5}Pr^{1/3} \text{ (Laminar boundary layer)} \tag{21}$$

$$Nu = 0.0292Re^{4/5}Pr^{1/3} \text{ (Turbulent boundary layer)} \tag{22}$$

where Pr is the Prandtl number, as defined by $Pr = \frac{c_\rho\mu}{\lambda}$.

The thermal conductivities of NH_4HCO_3 and NaCl can be obtained from Refs. [23] and [26].

Experimental

FO Membrane and Chemicals

The asymmetric FO membrane was obtained from Saehan (Republic of Korea). The porosity and tortuosity of support layer were 68.82% and 1.255, respectively, and the thicknesses of active and support layers were 1 and 100 μm, respectively. The FS was 0.5 mol/L sodium chloride solution, and the DS was 1.8 mol/L ammonium bicarbonate solution. All chemicals were of analytical grade and purchased from Jiangtian Chemical Reagent Co., Ltd (Tianjin, China).

FO Experiment

Figure 2 presents the schematic diagram of the FO experimental apparatus. It consisted of two stainless steel cells separated by an FO membrane. The length of the channel on the cell was 80 mm, the width was 40 mm, and the thickness was 3 mm, giving an effective area of 0.0032 m^2. The DS in the tank labeled as DS1 was heated by heater/cooler circulator, and flowed through the valve, pump, flow meter and pressure gage into the FO cell finally. In FO cell, the water molecules in FS were transported to DS driven by the osmotic pressure difference. The dilutive DS flowed through the pressure gage and valve into the tank labeled as DS5. The FS in the tank labeled as FS1 flowed into the tank labeled as FS5 in the same way. In the experiment, four tanks (DS1, DS5, FS1, FS5) were open, and four thermometers were placed in each tank to detect the solution temperatures. The FS and DS flowed through the two channels in the FO cell at a rate of 8.5 cm/s.

During each experimental period, the masses of FS in the tanks labeled FS1 (m_{FS1}) and FS5 (m_{FS5}) were detected by scale (XP32001LDR, Shanghai, China), respectively. At the end of each experiment, FS in the FS5 tank was collected to measure volume (V_F) with graduated cylinder, and the concentration of draw solute (C_{D1}) in it was analyzed by the portable parallel analyzer (SL1000, HACH, USA). In addition, DS in the DS5 tank was collected to detect the concentration of feed solute (C_{F5}) by ion chromatography (Thermo iCAP 7400, China). To ensure the accuracy of results, each experiment was repeated three times.

Evaluation of FO Performance

The performance of FO was evaluated by water flux (J_w) [27], the reverse draw solute flux (J_s) and the forward rejection of feed solute (R_F) [28], defined as:

Fig. 2 Schematic diagram of the FO experimental apparatus
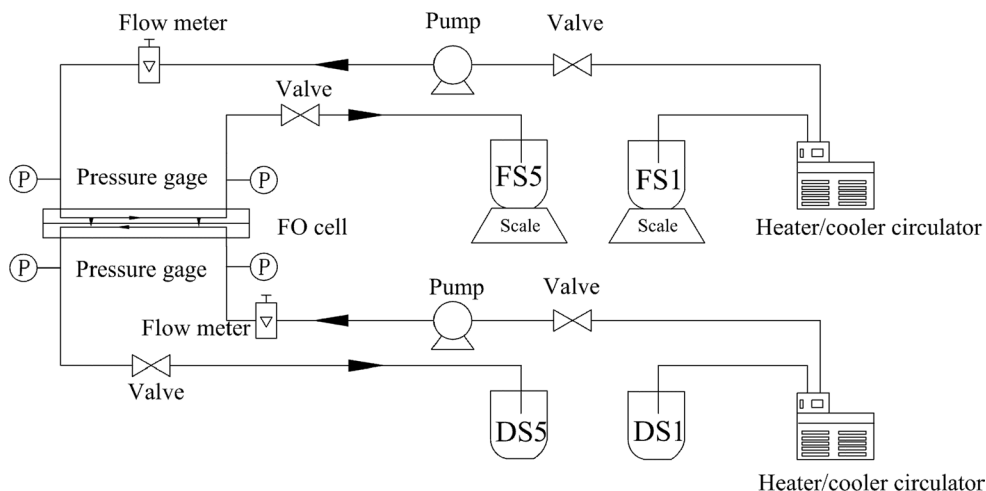
$$J_w = \frac{\Delta m}{\rho A_m \Delta t} \tag{23}$$

$$J_s = \frac{C_{D1} V_F}{A_m \Delta t} \tag{24}$$

$$R_F = \left(\frac{0.5 - C_{F5}}{0.5} \right) \times 100\% \tag{25}$$

where Δm is the mass change of FS, calculated by $m_F - m_{FS1} - m_{FS5}$, and m_F is the initial mass of FS; Δt is the time interval; and A_m is the area of FO membrane.

Results and Discussion

### Influence of Temperature on Membrane Permeation Coefficients

Fixing the DS temperature at a baseline (20 °C), the pure water flux as a function of additional hydraulic pressure at increased FS temperature (from 20 to 40 °C) is shown in Fig. 3a. Fixing the FS temperature at a baseline (20 °C), the pure water flux as a function of additional hydraulic pressure at increased DS temperature (from 20 to 40 °C) is shown in Fig. 3b. The slopes of these fitting lines represent values of water permeation coefficient at different temperature gradients, and the result indicates that the water permeation coefficient increases with an increase in the FS or DS temperature, which is consistent with previous research [29]. It should also be noticed that, by only increasing the FS temperature, the water permeation coefficient is higher than that by only increasing the DS temperature. Because the active layer of FO membrane is very dense, it is the main controlling factor in water flux. By only increasing the FS temperature, the temperature on the surface of active layer
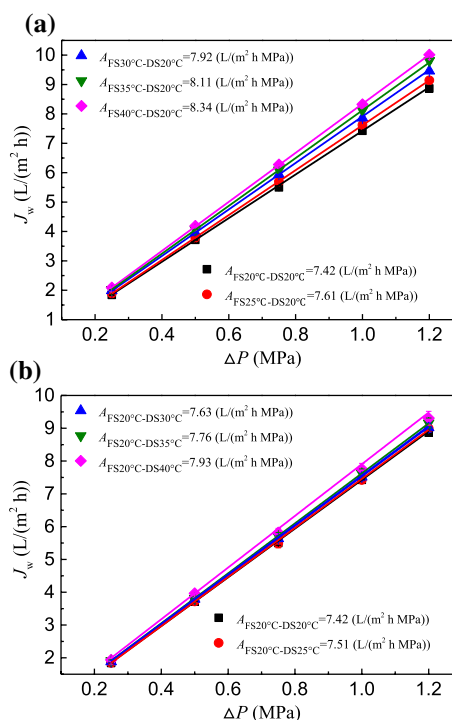
Fig. 3 Pure water flux as a function of additional hydraulic pressure when **a** DS temperature was fixed at 20 °C, and **b** FS temperature was fixed at 20 °C

(T_2) was higher than that by increasing the DS temperature only. And the water viscosity was lower and the water diffusion coefficient was larger at higher temperature, causing a larger water flux.

Figure 4 shows the variation of the NH_4HCO_3 permeation coefficient with FS or DS temperature when the temperature of DS or FS was fixed at 20 °C. The NH_4HCO_3 permeation coefficient increases with increasing FS or DS temperature, and only increasing the temperature of FS plays a more significant role than only increasing the DS
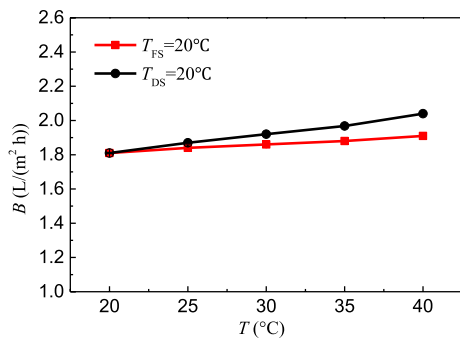
Fig. 4 Variation of NH_4HCO_3 permeation coefficient with FS or DS temperature

temperature. The biggest obstacle to the NH_4HCO_3 flux is also the active layer of FO membrane. Compared with only increasing the DS temperature, the temperature of the active layer was higher when only increasing the FS temperature. The higher temperature, the larger NH_4HCO_3 diffusion coefficient and the lower NH_4HCO_3 viscosity, the

higher NH_4HCO_3 flux, and the larger NH_4HCO_3 permeation coefficient.

Influence of Temperature on Membrane Structural Parameter

The membrane structural parameter (S) can be theoretically calculated by Eq. (9) using the water permeation coefficient (A), the NH_4HCO_3 permeation coefficient (B), the NH_4HCO_3 diffusion coefficient (D_{D5}), the NH_4HCO_3 osmotic pressure (π_{D5}), and water flux (J_w). Figure 5 shows the variation of the membrane structural parameter with the temperature of FS or DS. It was found that the membrane structural parameter decreased with an increase in the FS or DS temperature, which could be explained by the fact that the membrane porosity increased with an increase in the FS or DS temperature [30]. According to Eq. (9), the higher support layer porosity, the lower membrane structural parameter.
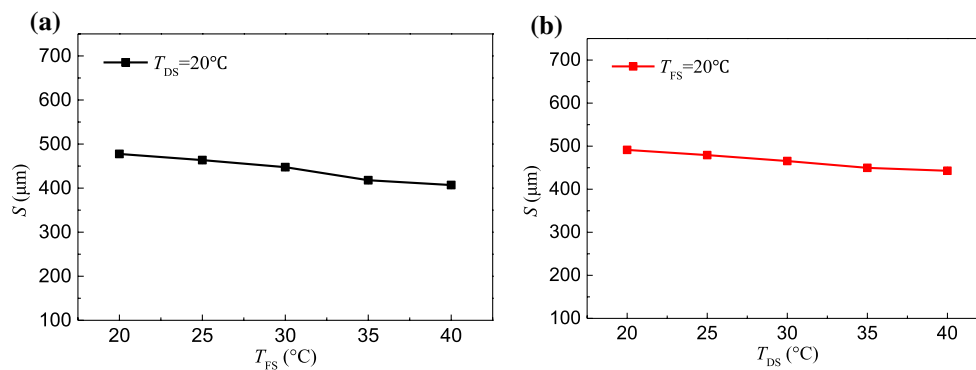
Fig. 5 Variation of the membrane structural parameter with **a** FS temperature, and **b** DS temperature
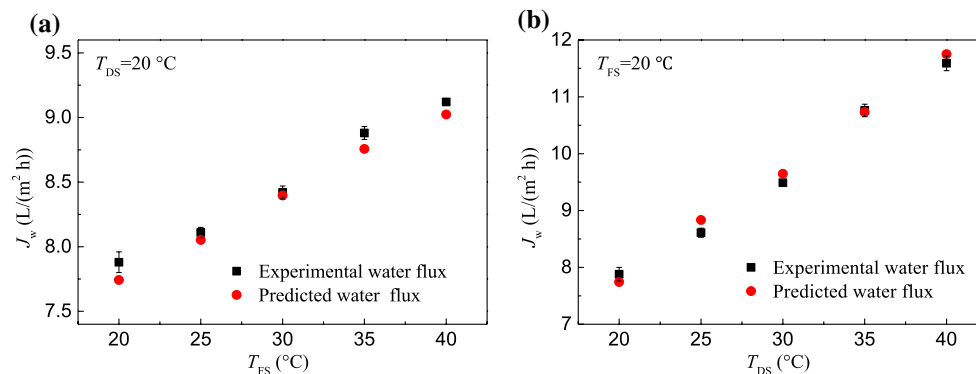
Fig. 6 Comparison between the predicted water flux and experimental water flux when **a** DS temperature was fixed at 20 °C, and **b** FS temperature was fixed at 20 °C

Influence of Temperature on FO Performance

Figure 6a shows the comparison between the predicted and experimental water flux data at the increased FS temperature (from 20 to 40 °C) when the temperature of DS was fixed at 20 °C. Figure 6b shows the comparison between the predicted and experimental water flux data at the increased DS temperature (from 20 to 40 °C) when the temperature of FS was fixed at 20 °C. The results demonstrated that the current model had a good accuracy of FO water flux.

Figure 6 also shows the effect of increasing FS or DS temperature on water flux in FO process. The water flux was enhanced significantly as increasing FS or DS temperature, and increasing the temperature of DS only played a more significant role than increasing FS temperature only. The percentage increase in water flux was 15.74% as increasing FS temperature from 20 to 40 °C, while it was 47.46% as increasing DS temperature from 20 to 40 °C. The water flux was determined by the water permeation coefficient and the effective osmotic pressure difference based on Eq. (1). As shown in Fig. 3, when the FS temperature increased from 20 to 40 °C, the percentage increase in water permeation coefficient was 12.40%, while it was just 6.87% when the DS temperature increased to 40 °C. When increasing the DS temperature, the NH_4HCO_3 diffusion coefficient is larger and the NH_4HCO_3 viscosity is lower, thereby resulting in a higher NH_4HCO_3 concentration and osmotic pressure at the interface between active layer and support layer (π_{D3}). By increasing the FS temperature from 20 to 40 °C, the percentage increase in the effective osmotic pressure difference ($\pi_{D3} - \pi_{F2}$) was 3.68%, while it was 42.00% as increasing the DS temperature to 40 °C. These results indicated that, compared with increasing the FS temperature, increasing the DS temperature was more significant to enhance the effective osmotic pressure difference, and a similar conclusion was obtained from Ref. [9]. In conclusion, the product of the water permeation coefficient and effective osmotic pressure

difference (the water flux) at increased DS temperature was higher than that at increased FS temperature.

Fixing the DS temperature at 20 °C, the comparison between experimental and predicted reverse NH_4HCO_3 fluxes at increased FS temperature (from 20 to 40 °C) is shown in Fig. 7a. Fixing the FS temperature at 20 °C, the comparison between experimental and predicted reverse NH_4HCO_3 fluxes at increased DS temperature (from 20 to 40 °C) is shown in Fig. 7b. The results showed that the current model was accurate in reverse NH_4HCO_3 flux prediction. In addition, it also showed that the reverse NH_4HCO_3 flux increased as increasing the FS or DS temperature, and the effect of only increasing the DS temperature was greater than that of only increasing the FS temperature. The percentage increase in reverse NH_4HCO_3 flux was 8.28% as elevating FS temperature from 20 to 40 °C, and 21.65% while elevating DS temperature from 20 to 40 °C. It can be explained as follows. According to Eq. (3), the reverse NH_4HCO_3 flux is positively correlated with the NH_4HCO_3 permeation coefficient and the concentration difference between C_{D3} and C_{D1}. According to Fig. 4, when the FS temperature increased from 20 to 40 °C, the percentage increase in the NH_4HCO_3 permeation coefficient was 10.87, and 5.52% while elevating DS temperature from 20 to 40 °C. According to Eqs. (8) and (10), the concentration difference between C_{D3} and C_{D1} was 2.72% by increasing the FS temperature from 20 to 40 °C, while 20.56% by increasing the DS temperature from 20 to 40 °C. Therefore, the product of the NH_4HCO_3 permeation coefficient and the concentration difference between C_{D3} and C_{D1} (the reverse NH_4HCO_3 flux) at increased DS temperature was higher than that at increased FS temperature.

Fixing DS temperature at 20 °C, the variation of NaCl rejection with FS temperature (from 20 to 40 °C) is shown in Fig. 8a. Fixing FS temperature at 20 °C, the variation of NaCl forward rejection with DS temperature (from 20 to 40 °C) is shown in Fig. 8b. The NaCl forward rejection increased with the increase in FS or DS temperature
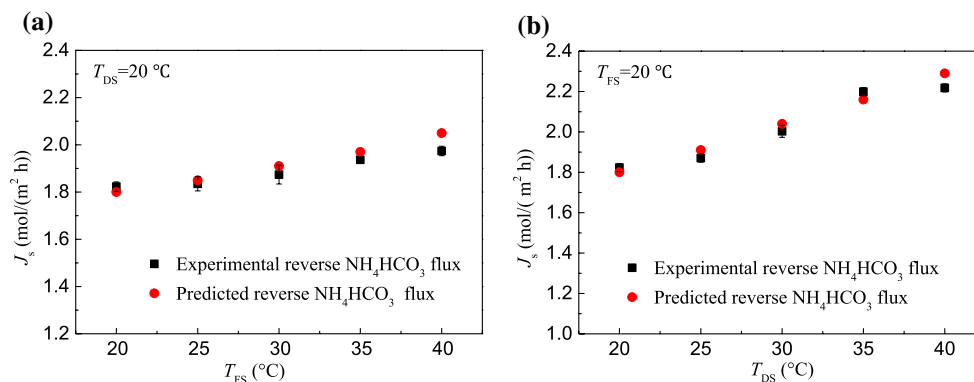
Fig. 7 Comparison between the predicted and experimental reverse NH_4HCO_3 fluxes when **a** DS temperature was fixed at 20 °C, and **b** FS temperature was fixed at 20 °C
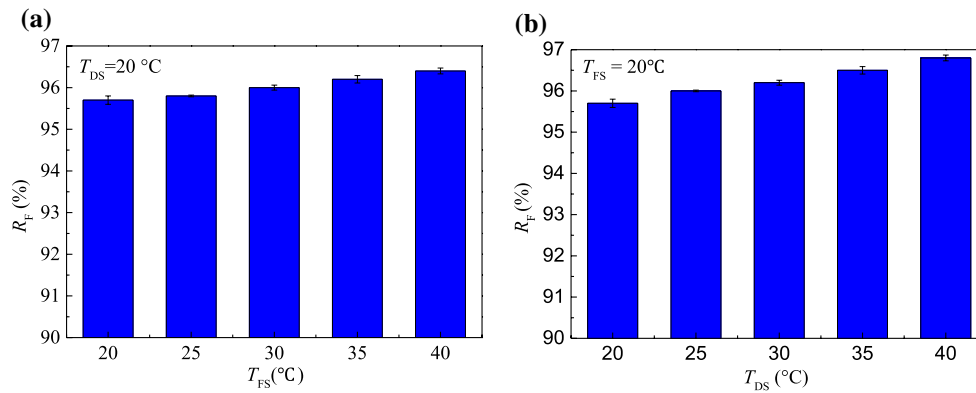
Fig. 8 Variation of NaCl rejection with **a** FS temperature, and **b** DS temperature

due to the dilution phenomenon, which has been extensively discussed in pressure-based membrane processes. And the increase in DS temperature also played a more significant role in NaCl forward rejection than that in FS temperature. The percentage increase in the NaCl forward rejection was 0.42% as only increasing the temperature of FS from 20 to 40 °C, and 1.15% as only increasing the temperature of DS from 20 to 40 °C. This difference is due to the higher water flux when only increasing the temperature of DS.

The most important criterion in designing FO system is the ratio of reverse draw solute flux to water flux, known as specific reverse solute flux (SRSF). A lower SRSF represents better FO performance. Figure 9a shows the variation in SRSF with FS temperature (from 20 to 40 °C) when the DS temperature was fixed at 20 °C, and Fig. 9b shows the variation of SRSF with DS temperature (from 20 to 40 °C) when the FS temperature was fixed at 20 °C. The SRSF decreased from 0.231 to 0.216 mol/L by only increasing the FS temperature from 20 to 40 °C, and the percentage decrease was 6.44%. In comparison, the SRSF decreased to 0.190 mol/L by only increasing the

DS temperature to 40 °C, and the percentage decrease was 17.50%. It indicates that, compared with increasing the FS temperature, increasing the DS temperature is more beneficial to reduce SRSF.

Conclusion

In order to investigate the influence of temperature on the performance of FO when the FS temperature was different from the DS temperature, a FO model considering the mass and heat transfers between FS and DS was developed. Using NH_4HCO_3 solution as DS, and NaCl solution as FS, relevant FO experiments were carried out. The predicted data using the current model coincided with those obtained from FO experiments.

When the temperature of FS or DS increased, water flux, forward rejection of feed solute, and reverse draw solute flux increased as well. When the FS temperature increased from 20 to 40 °C, the percentage increases in the water flux, the reverse NH_4HCO_3 flux, and NaCl forward rejection were 15.74%, 8.28%, and 0.42%, respectively, and 47.46%,
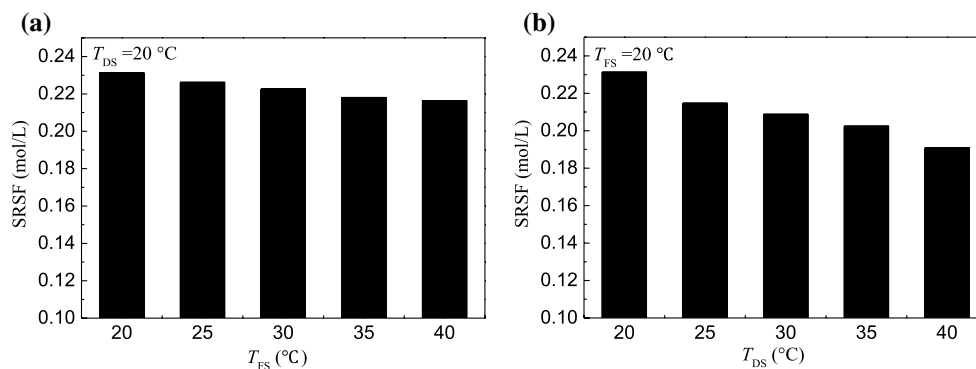
Fig. 9 Variation of SRSF with **a** FS temperature, and **b** DS temperature

21.65%, and 1.15% while increasing the DS temperature from 20 to 40 °C. Unilateral strengthening the DS temperature is more beneficial to improve FO performance.

References

1. Cheng HG, Wang SC (2007) Experimental investigation of modified polypropylene shell-tube column using humidification-dehumidification desalination process. Trans Tianjin Univ 13(3):181–185

2. Cath TY, Childress AE, Elimelech M (2006) Forward osmosis: principles, applications, and recent developments. J Membr Sci 281(1–2):70–87

3. Zhu S, Li M, El-Din MG (2017) Forward osmosis as an approach to manage oil sands tailings water and on-site basal depressurization water. J Hazard Mater 327:18–27

4. Chekli L, Kim JE, Saliby IE et al (2017) Fertilizer drawn forward osmosis process for sustainable water reuse to grow hydroponic lettuce using commercial nutrient solution. Sep Purif Technol 181:18–28

5. Phuntsho S, Shon HK, Majeed T et al (2012) Blended fertilizers as draw solutions for fertilizer-drawn forward osmosis desalination. Environ Sci Technol 46(8):4567–4575

6. Sant'Anna V, Marczak LDF, Tessaro IC (2012) Membrane concentration of liquid foods by forward osmosis: process and quality view. J Food Eng 111(3):483–489

7. Zhao S, Zou L (2011) Effects of working temperature on separation performance, membrane scaling and cleaning in forward osmosis desalination. Desalination 278:157–164

8. Nematzadeh M, Samimi A, Shokrollahzadeh S (2015) Application of sodium bicarbonate as draw solution in forward osmosis desalination: influence of temperature and linear flow velocity. Desalin Water Treat 12(3):1–8

9. Phuntsho S, Vigneswaran S, Kandasamy J et al (2012) Influence of temperature and temperature difference in the performance of forward osmosis desalination process. J Membr Sci 415–416:734–744

10. Hawari AH, Kamal N, Altaee A (2016) Combined influence of temperature and flow rate of feeds on the performance of forward osmosis. Desalination 398:98–105

11. You SJ, Wang XH, Zhong M et al (2012) Temperature as a factor affecting transmembrane water flux in forward osmosis: steady-state modeling and experimental validation. Chem Eng J 198–199:52–60

12. Suh C, Lee S (2013) Modeling reverse draw solute flux in forward osmosis with external concentration polarization in both sides of the draw and feed solution. J Membr Sci 427:365–374

13. Mcginnis RL, Hancock NT, Nowosielski-Slepowron MS et al (2013) Pilot demonstration of the NH_3/CO_2 forward osmosis desalination process on high salinity brines. Desalination 312:67–74

14. Hancock NT, Phillip WA, Elimelech M et al (2011) Bidirectional permeation of electrolytes in osmotically driven membrane processes. Environ Sci Technol 45(24):10642–10651

15. Loeb S, Titelman L, Korngold E et al (1997) Effect of porous support fabric on osmosis through a Loeb-Sourirajan type asymmetric membrane. J Membr Sci 129(2):243–249

16. Xu L, Lu WX, Xu W (2018) Modeling of computational fluid dynamics and experimental study of electro-catalytic oxidation enhanced nanofiltration for treating C.I. Acid Red 73 wastewater. Trans Tianjin Univ 24(2):123–130

17. Wang XS (1984) Concentration polarization in reverse osmosis and ultrafiltration. Chin J Chem Eng 35(2):157–163 **(in Chinese)**

18. Yong JS, Phillip WA, Elimelech M (2012) Coupled reverse draw solute permeation and water flux in forward osmosis with neutral draw solutes. J Membr Sci 392(2):9–17

19. Malta LFB (2002) Influence of crossflow membrane filter geometry and shear rate on colloidal fouling in reverse osmosis and nanofiltration separations. Environ Sci Technol 19(6):357–372

20. Tan CH, Ng HY (2008) Modified models to predict flux behavior in forward osmosis in consideration of external and internal concentration polarizations. J Membr Sci 324(1–2):209–219

21. Beijing Petrochemical Engineering, Co., Ltd (1988) Manual for physicochemical constants in chlor-alkali industry. Chemical Industry Press, Beijing **(in Chinese)**

22. Phillip WA, Yong JS, Elimelech M (2010) Reverse draw solute permeation in forward osmosis: modeling and experiments. Environ Sci Technol 44(13):5170–5176

23. Shi J, Wang JD, Yu GC et al (1996) Chemical engineering handbook. Chemical Industry Press, Beijing **(in Chinese)**

24. Wang WT, Liu SR (1990) Calculation of heat capacities for strong electrolyte solution. Chem Eng Des 1:48–54 **(in Chinese)**

25. Babu BR, Rastogi NK, Raghavarao KSMS (2008) Concentration and temperature polarization effects during osmotic membrane distillation. J Membr Sci 322(1):146–153

26. Ozbek H, Phillips SL (1980) Thermal conductivity of aqueous sodium chloride solutions from 20 to 330 °C. J Chem Eng Data 25(3):263–267

27. Ban R, Liu M, Qin Y et al (2012) Enrichment of semi-volatile organic acids from aqueous solutions by multiple-effect membrane distillation. Trans Tianjin Univ 18(5):320–329

28. Chen Y, Jia W, Hu J et al (2017) Performance of catalytically active membrane reactors with different A/V ratios. Trans Tianjin Univ 23(6):521–529

29. Ming X, Price WE, Long DN et al (2013) Effects of feed and draw solution temperature and transmembrane temperature difference on the rejection of trace organic contaminants by forward osmosis. J Membr Sci 438:57–64

30. Goosen MFA, Sablani SS, Al-Maskari SS et al (2002) Effect of feed temperature on permeate flux and mass transfer coefficient in spiral-wound reverse osmosis systems. Desalination 144(1):367–372